Section: Miscellaneous

Original Research Article

POLYPHENOLIC PHYTOCHEMICALS OF ALSTONIA MACROPHYLLA AS INHIBITORS OF SODIUM-GLUCOSE CO-TRANSPORTER-2 (SGLT-2) IN THE TREATMENT OF TYPE 2 DIABETES MELLITUS – AN IN-SILICO STUDY

Nivedhitha Piruthivirajan[1], K. P. Eshwaanth Keerthi[2], Murali Shanmugam[3], K. Piruthivirajan[4], Maruthupandian[5]

[1]MBBS, Tagore Medical College and Hospital, Rathinamangalam, Chennai, India.
[2]M.B.B.S., Bhaarath Medical College and Hospital, Selaiyur. Chennai, India.
[3]Professor, Tagore Medical College and Hospital, Rathinamangalam, Chennai., India.
[4]Professor, Sri Lakshmi Narayana Institute of Medical Sciences, Pondicherry, India.
[5]Associate Professor, Tagore Medical College and Hospital, Rathinamangalam, Chennai, India.

Received : 08/04/2025
Received in revised form : 03/06/2025
Accepted : 25/06/2025

Keywords:
SGLT2 Inhibitors, Alstonia macrophylla, Molecular docking.

Corresponding Author:
Dr. Nivedhitha Piruthivirajan,
Email: dr.k.p.r.navalur@gmail.com

DOI: 10.47009/jamp.2025.7.4.20

Source of Support: Nil,
Conflict of Interest: None declared

Int J Acad Med Pharm
2025; 7 (4); 100-107

ABSTRACT

Diabetes is a chronic medical condition in which bloodstream glucose levels increase. In Type 2 diabetes mellitus, the cells cannot utilize blood glucose as cells have become resistant to pancreatic insulin gradually increasing blood glucose levels. One of the latest advancements in the treatment of diabetes is by the inhibition of sodium-glucose co-transporter protein located in the kidney proximal tubule which leads to a decrease in blood glucose by increasing renal glucose excretion. Gliflozins, are a new class of diabetic medications with SGLT2 inhibiting properties indicated for diabetes treatment. They have shown cardiac benefits by reducing blood pressure, causing weight loss and reducing the risk of death from cardiovascular causes. By identifying potential SGLT-2 inhibitors within Alstonia macrophylla, a tree native to South East Asia known to be a rich source of Phlorizin a Gliflozin, this research aims to contribute to the development of novel, natural therapies for the management of type 2 diabetes through docking-based in-silico approach. Molecular docking of 150 derivatives of Alstonia macrophylla with SGLT2 was conducted using Autodock Vina in PyRx to determine binding efficacy. The three-dimensional structure of Human SGLT2-MAP17 in complex with long-acting inhibitor Empagliflozin (PDB CODE: 7VSI) was obtained from RCSB –protein database. The structures of 3 ligands of A.macrophylla, Alstiphyllanine A, Alstiphyllanine H and Picrinine were obtained from PubChem. Using ACD/ChemSketch, 50 ligand derivatives of Alstiphyllanine A, Alstiphyllanine H and Picrinine were generated. Results pointed out that six ligands, had efficient combating action against SGLT2 with lower binding energy than Empagliflozin, tightly adhering to the binding site of SGLT2. Besides, pharmacokinetic properties and toxicity profiles evaluated using Swiss ADME and ADMETSAR proved these 6 ligands had appreciable physiochemical properties, satisfying Lipinski's rule of 5 and had acceptable ADMET profiles. Thus, these compounds have showed promising results and could be considered potential drug candidates.

INTRODUCTION

In 2017, The International Diabetes Federation (IDF) measured that around 451 million people had diabetes and estimated the number to increase to 693 million by 2045, which leads to a large social, financial, and health system burden.[1] Devastating vascular complications of both the macro- and microvascular systems (cardiovascular disease, diabetic retinopathy, nephropathy, neuropathy) are the leading cause of morbidity and mortality in individuals with diabetes, causing blindness, kidney failure and overall decreased quality of life which carries enormous financial burden with unequal healthcare expenditure and access to treatment between developed and developing countries.[1-6]

Diabetes is a chronic metabolic disorder characterized by high blood glucose levels due to beta-cell dysfunction causing insulin deficiency or due to insulin resistance or both. It is classically

ISSN (O): 2687-5365; ISSN (P): 2753-6556

divided into an early-onset autoimmune form (type 1 diabetes or T1D) which is due to insufficient insulin production, a late-onset non-autoimmune form (T2D) which is due to insensitivity to insulin, monogenic diabetes (e.g. Maturity-onset Diabetes of the Young [MODY] or neonatal diabetes and gestational diabetes).[2] Patients with Type 2 DM have impaired glucose tolerance due to insulin resistance in which the pancreas still makes insulin but the cells cannot use blood glucose efficiently for energy. Measures of β-cell function and insulin sensitivity in type 2 DM are significantly impaired resulting in an increase in the plasma glucose levels which are underutilized and excreted in urine.[3]

The kidney re-absorbs approximately 180 g of filtered glucose per day.[4] SGLT proteins are transporters of glucose, located in the small intestines and the proximal tubule of the kidneys. SGLT1 plays a role in intestinal glucose re-absorption and a lesser role in glucose re-absorption in the renal tubules. Its inhibition may lead to gastrointestinal complications, including severe diarrhea.[2] SGLT2 is a transporter in the early portion of the proximal renal tubule. The majority of renal glucose re-absorption (up to 90%) is mediated by SGLT2. The normal renal threshold for re-absorption of glucose is 180 mg/dl,[4] all of it being reabsorbed and less than 1% being excreted in the urine.[3] When the blood glucose levels escalate, capacity of the kidney to reabsorb glucose is exceeded and excess glucose is excreted in urine.

In Type 2 DM, due to the increased blood glucose levels, the kidney tries to compensate for the increased filtered load of glucose by increasing the expression of SGLT2 proteins increasing its ability to reabsorb glucose into the plasma, further exacerbating hyperglycemia. Therefore renal glucose threshold is increased up to ~240mg/dL.[3]

Inhibition of SGLT2 proteins can reduce this threshold to 40–120 mg/dl.[4] Thus, SGLT2 inhibitors function by inhibiting the SGLT2 transporter in the proximal tubule of the kidney which causes glucosuria. This produces a reduction in blood glucose.[4]

An alkaloid, Phlorizin was identified as a nonspecific inhibitor of SGLT proteins.[3] Currently, three SGLT2 selective inhibitors derivatives of phlorizin have been approved by the FDA canagliflozin, dapagliflozin, and empagliflozin. Other SGLT2 inhibitors, ipragliflozin, ertugliflozin, luseogliflozin, and tofogliflozin are in various stages of clinical development.[3]

The advantages of SGLT2 inhibitor class of drugs is that they are useful in obese and hypertensive patients because of their weight loss, antihypertensive and cardiovascular benefits, they reduce mortality from heart failure and have kidney protective properties.[4] In clinical trials of SGLT2 inhibitors, a weight loss of approximately 1–4 kg occurred over 18–104 weeks.[4] Significant reductions in BP are believed to be due to the diuretic and volume depletion effects, inhibition of the renin–angiotensin system and weight loss.[2] A modest but statistically significant increase in both high-density lipoprotein (HDL) and low-density lipoprotein (LDL) cholesterol has also been observed.[4]

SGLT2 inhibitors are contraindicated for patients with renal insufficiency. It has also been associated with a slight increase in the incidence of urinary tract infections as glucose in the urine can facilitate the onset of mycotic infections.[4] The osmotic diuresis induced by glycosuria resulting from SGLT2 inhibition, leads to polyuria, postural dizziness, orthostatic hypertension and polydipsia.[3,4] According to a study, SGLT2 inhibitors increased risk of acute kidney injury (AKI), particularly when combined with NSAIDs, anti-RAS, or diuretics. There is evidence that dapagliflozin contributes to the advancement of renal dysfunction.[5] Post-marketing studies indicate an increased incidence of adverse effects such as diabetic ketoacidosis, cancer, bone fracture, foot and leg amputation. SGLT2 inhibitors decrease urinary excretion of ketone bodies thereby increasing the plasma ketone body levels causing diabetic ketoacidosis.[6] Thus, there is a need for better understanding the risk profile of SGLT2 inhibitors.[7]

SGLT 2 inhibitors currently available in market have the above-mentioned adverse effects. Thus, there is an urgent need to develop plant-based inhibitors which can overcome these drawbacks. Alstonia macrophylla, a tree native to the South East Asian countries India, Indonesia, Malaysia and Sri Lanka is discovered to be a source of phlorizin. It is found to be a rich source of alkaloids with various anti-cancerous, anti-bacterial, anti-inflammatory and anti-tussive properties.[8] The derivatives of alkaloids from Alstonia macrophylla, Alstiphyllanine A, Alstiphyllanine H and Picrinine can be efficiently used as alternative drugs.

Objective

1. To perform Molecular docking of the polyphenolic phytochemicals from Alstonia macrophylla with SGLT-2 to determine its binding efficacy
2. To determine the ADMET properties of Alstonia macrophylla polyphenols by an in-Silico method.

MATERIALS AND METHODS

Molecular docking is the study tool used in this study. It aims in designing potential drugs by appropriate binding of target protein and ligand with minimum binding energy using computer assisted software.

This study was done in the bio informatics facility, Central Research lab of our college.[9]

Target Protein preparation: The three-dimensional structure of Human sodium Glucose Co-Transporter 2, SGLT2-MAP17 in complex with long-acting inhibitor empagliflozin (PDB CODE: 7VSI) was obtained from RCSB –protein database in PDB format. The 3D structure of SGLT2-MAP17 in complex with long-acting inhibitor empagliflozin is shown in the [Figure 1]. Alpha helices are colored

ISSN (O): 2687-5365; ISSN (P): 2753-6556

yellow, Beta sheets are green, turns are green and other residues are white.

Figure 1: The 3D structure of SGLT2-MAP17 in complex with long-acting inhibitor empagliflozin (PDB CODE: 7VSI)

Ligand preparation: The structure of 3 ligands, Alstiphyllanine A, Alstiphyllanine H and Picrinine was obtained from PubChem database.

1. Alstiphyllanine A

Other details of compound were also obtained from PubChem database.
Compound PubChem CID: 45268837
MF: C24H28N2O5
MW: 424.5g/mol
IUPAC Name: methyl (1R,9S, 10S, 12S, 13Z, 16S, 17R, 18S)-18-acetyloxy-13-ethylidene-8-methyl-15-oxido-8-aza-15-azoniahexacyclo [14.2.1.01, 9.02, 7.010, 15.012, 17] nonadeca-2,4,6-triene-17-carboxylate

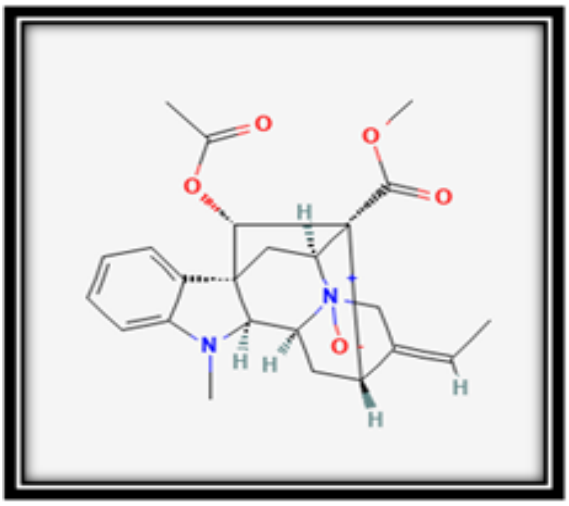

Figure 2: Structure of Alstiphyllanine A

2. Alstiphyllanine H:

The structure of Alstiphyllanine H was obtained from PubChem database. Other details of the compound were also obtained from PubChem database.
Compound PubChem CID is 46229074.
MF: C22H26N2O4
MW: 382.5
IUPAC Name: methyl (1R, 9S, 10S, 12S, 13Z, 16S, 17S)-13-ethylidene-18-hydroxy-8-methyl-15-oxido-8-aza-15-azoniahexacyclo [14.2.1.01, 9.02, 7.010, 15.012, 17] nonadeca-2,4,6-triene-17-carboxylate

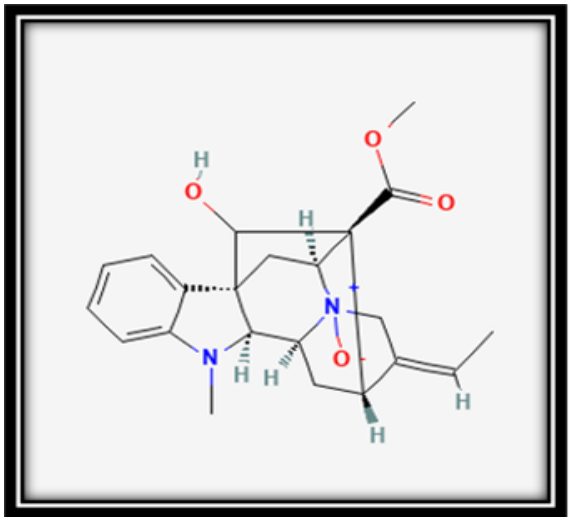

Figure 3: Structure of Alstiphyllanine H

3. Picrinine

The structure of Picrinine was obtained from PubChem database. Other details of the compound were also obtained from PubChem database.
Compound PubChem CID is 5478940
MF: C20h22n2o3
MW: 338.4
IUPAC Name: methyl (14Z)-14-ethylidene-18-oxa-2,12-diazahexacyclo [9.6.1.19, 15.01, 9.03, 8.012, 17] nonadeca-3,5,7-triene-19-carboxylate.

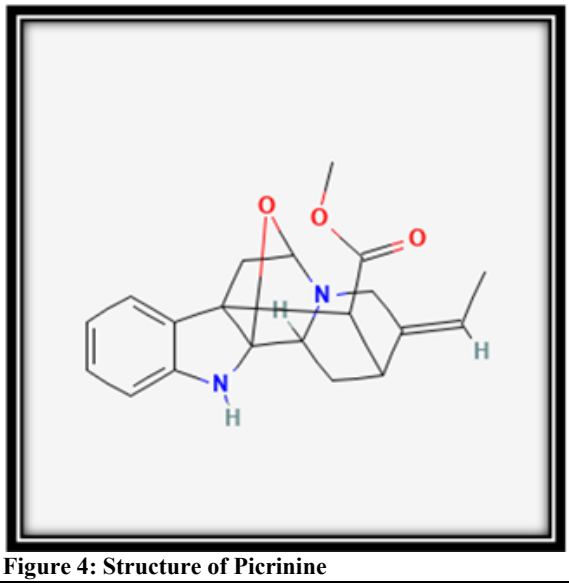

Figure 4: Structure of Picrinine

Protein Ligand Binding: 50 ligand derivatives of Alstiphyllanine A, 50 ligand derivatives od Alstiphyllanine H and 50 ligand derivatives of Picrinine were generated by software

ISSN (O): 2687-5365; ISSN (P): 2753-6556

ACD/ChemSketch(10). Ligands were converted from mol 2 format to PDB format using OPEN BABEL software. Accurate docking of the derivatives with SGLT2 was performed using Autodock Vina in PyRx.[11] The derivatives with least binding energy were selected and their pharmacokinetic properties and toxicity profile were evaluated using SwissADME and ADMETSAR.[12]

Visualization: The docking pose of Alstiphyllanine A, Alstiphyllanine H and Picrinine and its derivatives were visualized using software Biovia Discovery Studios. Its BMP (Bitmap image) was used to check the rotatability of all the bonds. The H-bonds and its lengths were visualized using the same software.

RESULTS

150 derivatives of the alkaloids Alstiphyllanine A, Alstiphyllanine H and Picrinine were prepared and rough docking was done, of which six derivatives with highest total binding energy (kcal/mol) were selected.

Table 1: The results of rough docking using AutodockVina in PyRx showing binding energies of the 6 derivatives of Alstiphyllanine A, Alstiphyllanine H and Picrinine with SGLT2

Sr. No.	Ligand	Total binding energy(kcal/mol)	Vander Waals force	Conventional H-Bond	Carbon H-Bonds
1	(1R,9S,10R,12S,13Z,15S,16R,17R,18R)-18-[(2-aminoethanimidoyl)oxy]-13-(2-aminopropylidene)-17-(methoxycarbonyl)-4,5,8-trimethyl-8,15-diazahexacyclo[14.2.1.0^{1},^{9}.0^{2},^{7}.0^{10},^{15}.0^{12},^{17}]nonadeca-2(7),3,5-trien-15-ium-15-olate	-6.7	11	2	1
2	(1R,9S,10R,12S,13Z,15S,16R,17R,18S)-13-ethylidene-18-hydroxy-18-(hydroxymethyl)-3,4,8-trimethyl-17-[(trihydroxymethoxy)methanimidoyl]-8,15-diazahexacyclo[14.2.1.0^{1},^{9}.0^{2},^{7}.0^{10},^{15}.0^{12},^{17}]nonadeca-2(7),3,5-trien-15-ium-15-olate	-8.7	6	4	0
3	aminomethyl (1S,9R,11R,14E,15R,17R,19R)-4,5,6-triamino-14-ethylidene-18-oxa-2,12-diazahexacyclo[9.6.1.1^{9},^{15}.0^{1},^{9}.0^{3},^{8}.0^{12},^{17}]nonadeca-3(8),4,6-triene-19-carboxylate	-8	10	4	1
4	hydrazinylmethyl (1S,9R,11R,14E,15R,17R,19R)-14-ethylidene-4,7-dihydroxy-18-oxa-2,12-diazahexacyclo[9.6.1.1^{9},^{15}.0^{1},^{9}.0^{3},^{8}.0^{12},^{17}]nonadeca-3(8),4,6-triene-19-carboxylate	-8.6	13	1	2
5	trihydroxymethyl 14-acetyl-4-methyl-18-oxa-2,12-diazahexacyclo[9.6.1.1^{9},^{15}.0^{1},^{9}.0^{3},^{8}.0^{12},^{17}]nonadeca-3,5,7-triene-19-carboxylate	-9.2	11	2	0
6	hydroxymethyl (14E)-14-ethylidene-5-hydroxy-18-oxa-2,12-diazahexacyclo[9.6.1.1^{9},^{15}.0^{1},^{9}.0^{3},^{8}.0^{12},^{17}]nonadeca-3,5,7-triene-19-carboxylate	-8.5	10	2	1

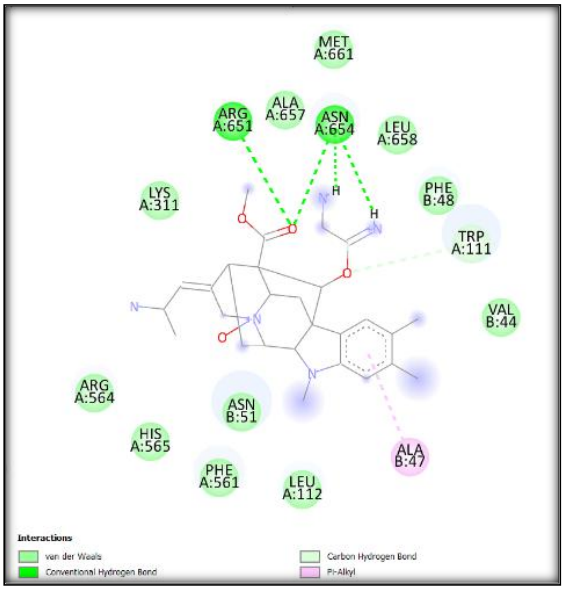

Figure 5: Interactions of SGLT2 with selected ligands:

1. (1R, 9S, 10R, 12S, 13Z, 15S, 16R, 17R, 18R)-18-[(2-aminoethanimidoyl) oxy] -13-(2-aminopropylidene) -17-(methoxycarbonyl)-4, 5, 8-trimethy l-8, 15-diazahexacyclo [14.2.1.0^{1},^{9} .0^{2},^{7}.0^{10},^{15} .0^{12},^{17}] nonadeca-2(7),3,5-trien-15-ium-15-olate

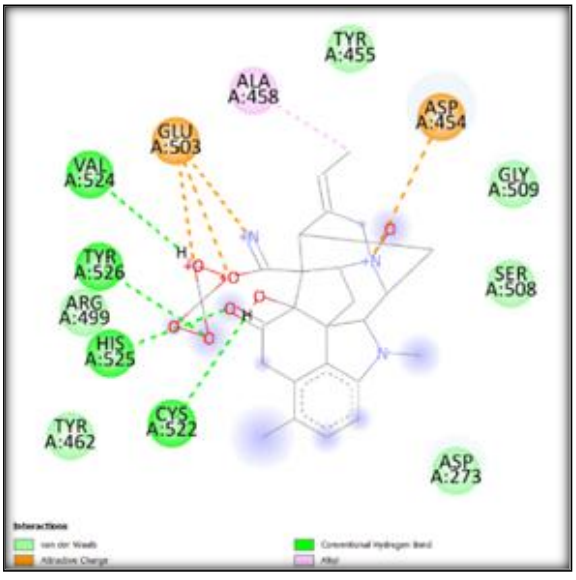

ISSN (O): 2687-5365; ISSN (P): 2753-6556

2. (1R, 9S, 10R, 12S, 13Z, 15S, 16R, 17R, 18S) -13-ethylidene -18-hydroxy-18-(hydroxymethyl)-3,4, 8-trimethy l-17- [(trihydroxymethoxy) methanimidoyl]-8,15-diazahexacyclo [14.2.1.0^{1,9} .0^{2,7}.0^{10,15}.0^{12,17}] nonadeca-2(7),3,5-trien-15-ium-15-olate

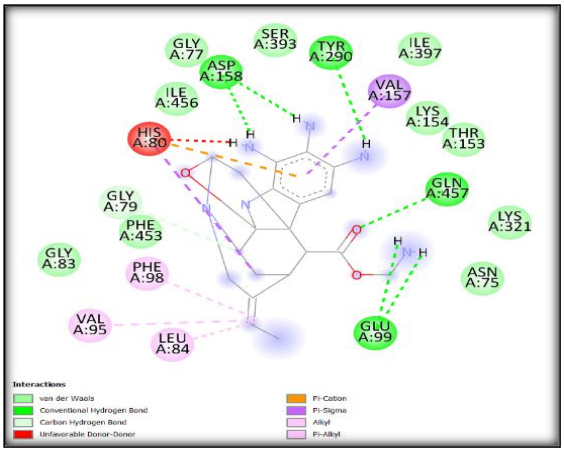

3. Aminomethyl (1S,9R,11R,14E,15R,17R,19R)-4, 5, 6-triamino-14-ethylidene -18-oxa-2, 12-diazahexacyclo [9.6.1.1^{9},^{15}.0^{1},^{9}.0^{3},^{8}.0^{12},^{17}] nonadeca-3(8), 4,6-triene-19-carboxylate

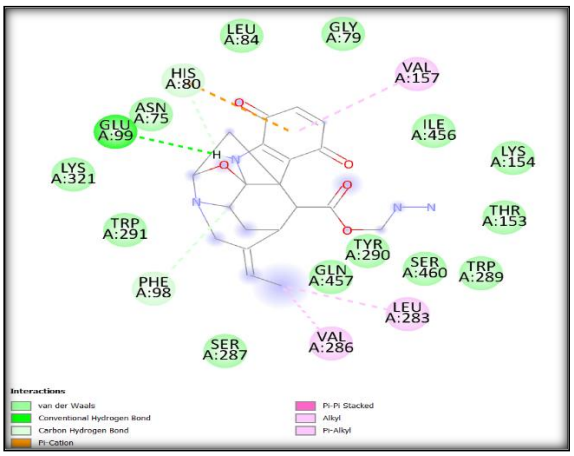

4. Hydrazinylmethyl (1S, 9R, 11R, 14E, 15R, 17R, 19R) -14-ethylidene-4,7-dihydroxy-18-oxa-2,12-diazahexacyclo[9.6.1.1^{9},^{15}.0^{1},^{9}.0^{3},^{8}.0^{12},^{17}]nonadeca-3(8),4,6-triene-19-carboxylate

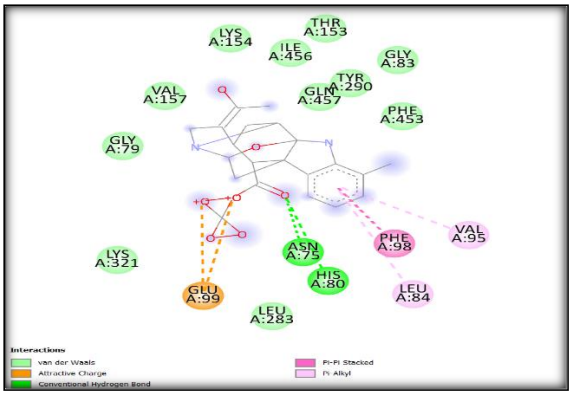

5. trihydroxymethyl 14-acetyl-4-methyl-18-oxa-2,12-diazahexacyclo [9.6.1.1^{9},^{15}.0^{1},^{9}.0^{3},^{8}.0^{12},^{17}] nonadeca-3,5,7-triene-19-carboxylate.

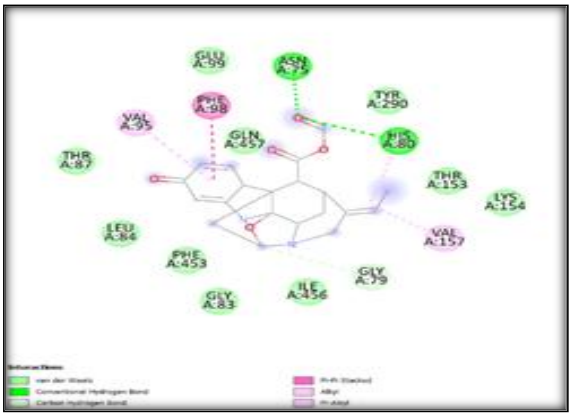

6. hydroxymethyl (14E)-14-ethylidene-5-hydroxy -18-oxa-2, 12-diazahexacyclo [9.6.1.1^{9},^{15}.0^{1},^{9} .0^{3},^{8}.0^{12},^{17}] nonadeca-3,5,7-triene-19-carboxylate

Figure 6: The structure and IUPAC name of the 6 derivatives of Alstiphyllanine A, Alstiphyllanine H and Picrinine with SGLT2

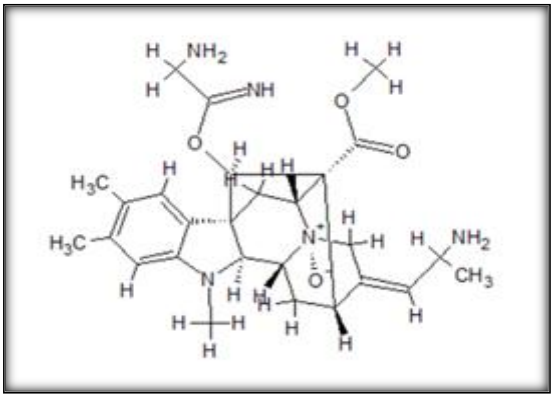

1. (1R,9S,10R,12S,13Z,15S,16R,17R,18R)-18-[(2-aminoethanimidoyl) oxy]- 13-(2-aminopropylidene)- 17-(methoxycarbonyl)-4,5, 8-trimethy l-8,15-diazahexacyclo [14.2.1.0^{1},^{9}.0^{2},^{7}.0^{10},^{15}.0^{12},^{17}] nonadeca-2(7),3,5-trien-15-ium-15-olate.

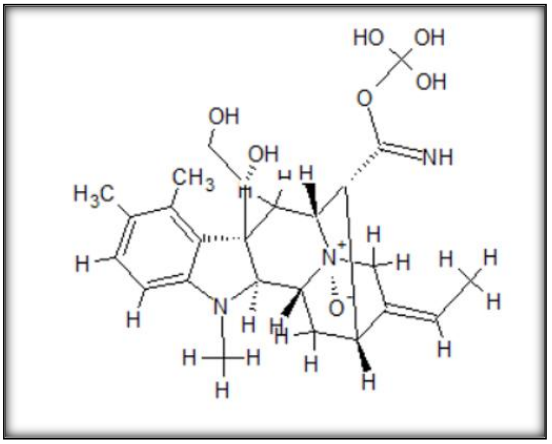

2. (1R,9S,10R,12S,13Z,15S,16R,17R,18S)- 13-ethylidene -18-hydroxy-18-(hydroxymethyl)-3,4,8- trimethyl-17-[(trihydroxymethoxy) methanimidoyl] -8,15-diazahexacyclo [14.2.1.0^{1},^{9} .0^{2},^{7}.0^{10},^{15}.0^{12},^{17}] nonadeca-2(7),3,5-trien-15-ium-15-olate.

ISSN (O): 2687-5365; ISSN (P): 2753-6556

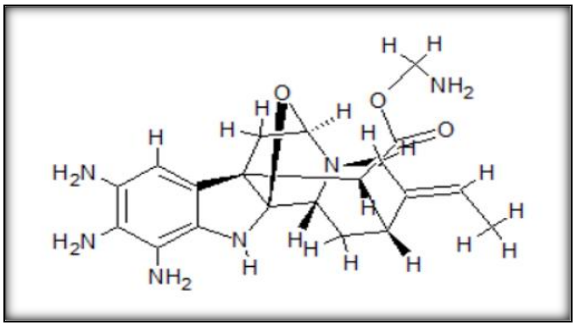

3. Aminomethyl(1S,9R,11R,14E,15R,17R,19R)-4, 5, 6-triamino -14-ethylidene-18-oxa-2, 12 diazahexacyclo [9.6.1.1^{9},^{15} .0^{1},^{9}.0^{3},^{8}.0^{12},^{17}] nonadeca-3(8), 4, 6-triene-19-carboxylate

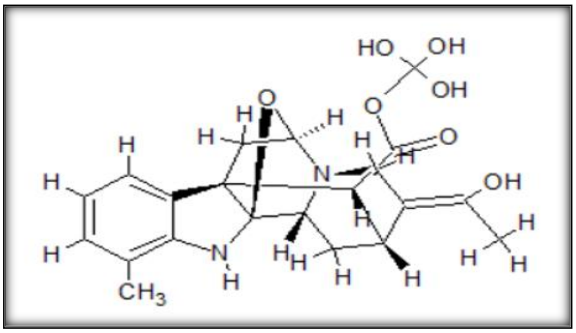

5. trihydroxymethyl 14-acetyl-4-methyl-18-oxa-2, 12-diazahexacyclo [9.6.1.1^{9},^{15} .0^{1},^{9}.0^{3},^{8} .0^{12},^{17}] nonadeca-3,5,7-triene-19-carboxylate

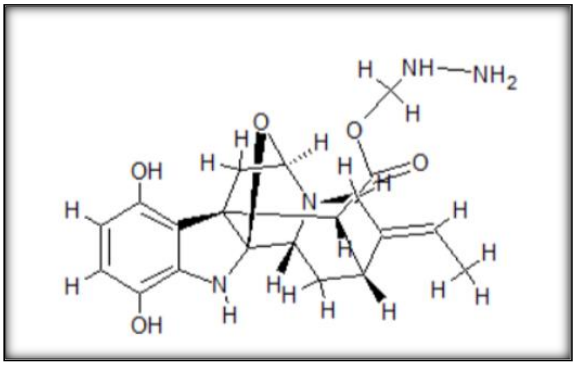

4. Hydrazinylmethyl (1S, 9R, 11R, 14E, 15R, 17R, 19R) -14-ethylidene-4,7-dihydroxy-18-oxa-2,12-diazahexacyclo[9.6.1.1^{9},^{15}.0^{1},^{9}.0^{3},^{8}.0^{12},^{17}]nonadeca-3(8),4,6-triene-19-carboxylate

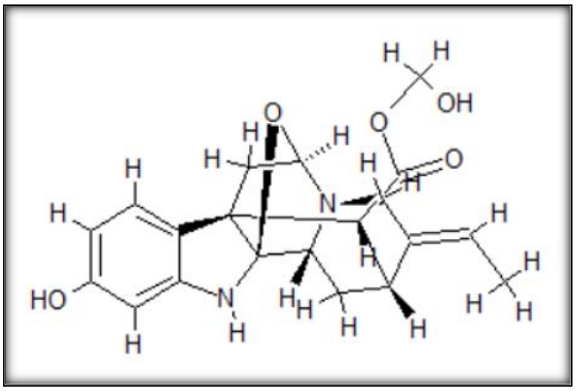

6. hydroxymethyl (14E)-14-ethylidene-5-hydroxy-18-oxa-2,12-diazahexacyclo [9.6.1.1^{9},^{15} .0^{1},^{9} .0^{3},^{8} .0^{12},^{17}] nonadeca-3,5,7-triene-19-carboxylate.

Table 2: The results of accurate docking using Autodock Vina in PyRx showing binding affinities of the 6 derivatives of Alstiphyllanine A, Alstiphyllanine H and Picrinine with SGLT2

No.	Ligands	Total Binding Affinity (kcal/mol)	Mode	RMSD Lower bond	RMSD Upper Bond
1.	(1R,9S,10R,12S,13Z,15S,16R,17R,18R)-18-[(2-aminoethanimidoyl)oxy]-13-(2-aminopropylidene)-17-(methoxycarbonyl)-4,5,8-trimethyl-8,15-diazahexacyclo[14.2.1.0^{1},^{9}.0^{2},^{7}.0^{10},^{15}.0^{12},^{17}]nonadeca-2(7),3,5-trien-15-ium-15-olate	-6.7	0	0	0
2.	(1R,9S,10R,12S,13Z,15S,16R,17R,18S)-13-ethylidene-18-hydroxy-18-(hydroxymethyl)-3,4,8-trimethyl-17-[(trihydroxymethoxy)methanimidoyl]-8,15-diazahexacyclo[14.2.1.0^{1},^{9}.0^{2},^{7}.0^{10},^{15}.0^{12},^{17}]nonadeca-2(7),3,5-trien-15-ium-15-olate	-8.7	0	0	0
3.	aminomethyl (1S,9R,11R,14E,15R,17R,19R)-4,5,6-triamino-14-ethylidene-18-oxa-2,12-diazahexacyclo[9.6.1.1^{9},^{15}.0^{1},^{9}.0^{3},^{8}.0^{12},^{17}]nonadeca-3(8),4,6-triene-19-carboxylate	-8	0	0	0
4.	hydrazinylmethyl (1S,9R,11R,14E,15R,17R,19R)-14-ethylidene-4,7-dihydroxy-18-oxa-2,12-diazahexacyclo[9.6.1.1^{9},^{15}.0^{1},^{9}.0^{3},^{8}.0^{12},^{17}]nonadeca-3(8),4,6-triene-19-carboxylate	-8.6	0	0	0
5.	trihydroxymethyl 14-acetyl-4-methyl-18-oxa-2,12-diazahexacyclo[9.6.1.1^{9},^{15}.0^{1},^{9}.0^{3},^{8}.0^{12},^{17}]nonadeca-3,5,7-triene-19-carboxylate	-9.2	0	0	0
6.	hydroxymethyl (14E)-14-ethylidene-5-hydroxy-18-oxa-2,12-diazahexacyclo[9.6.1.1^{9},^{15}.0^{1},^{9}.0^{3},^{8}.0^{12},^{17}]nonadeca-3,5,7-triene-19-carboxylate	-8.5	0	0	0

Table 3: The hydrogen bonds, its length, the amino acid residues and its position in the protein involved in the hydrogen bond formation for each ligand docking

Sr. No.	Ligand	Amino Acid residue involved in the hydrogen bond formation
1.	(1R,9S,10R,12S,13Z,15S,16R,17R,18R)-18-[(2-aminoethanimidoyl)oxy]-13-(2-aminopropylidene)-17-(methoxycarbonyl)-4,5,8-trimethyl-8,15-diazahexacyclo[14.2.1.0^{1},^{9}.0^{2},^{7}.0^{10},^{15}.0^{12},^{17}]nonadeca-2(7),3,5-trien-15-ium-15-olate	ARGA:651
		ASN A:654
		TRP A:111
2.		VAL A:524

ISSN (O): 2687-5365; ISSN (P): 2753-6556

	(1R,9S,10R,12S,13Z,15S,16R,17R,18S)-13-ethylidene-18-hydroxy-18-(hydroxymethyl)-3,4,8-trimethyl-17-[(trihydroxymethoxy)methanimidoyl]-8,15-diazahexacyclo[14.2.1.0^{1},^{9}.0^{2},^{7}.0^{10},^{15}.0^{12},^{17}]nonadeca-2(7),3,5-trien-15-ium-15-olate	TYR A:526
		HIS A:525
		CYS A:522
3.	aminomethyl (1S,9R,11R,14E,15R,17R,19R)-4,5,6-triamino-14-ethylidene-18-oxa-2,12-diazahexacyclo[9.6.1.1^{9},^{15}.0^{1},^{9}.0^{3},^{8}.0^{12},^{17}]nonadeca-3(8),4,6-triene-19-carboxylate	GLY A:79
		GLU A:99
		GLN A:457
		TYR A:290
		ASP A:158
4.	hydrazinylmethyl (1S,9R,11R,14E,15R,17R,19R)-14-ethylidene-4,7-dihydroxy-18-oxa-2,12-diazahexacyclo[9.6.1.1^{9},^{15}.0^{1},^{9}.0^{3},^{8}.0^{12},^{17}]nonadeca-3(8),4,6-triene-19-carboxylate	HIS A:80
		PHE A:98
		GLU A:99
5.	trihydroxymethyl 14-acetyl-4-methyl-18-oxa-2,12-diazahexacyclo[9.6.1.1^{9},^{15}.0^{1},^{9}.0^{3},^{8}.0^{12},^{17}]nonadeca-3,5,7-triene-19-carboxylate	ASN A:75
		HIS A:80
6.	hydroxymethyl (14E)-14-ethylidene-5-hydroxy-18-oxa-2,12-diazahexacyclo[9.6.1.1^{9},^{15}.0^{1},^{9}.0^{3},^{8}.0^{12},^{17}]nonadeca-3,5,7-triene-19-carboxylate	ASN A:75
		HIS A:80
		GLY A:79

Table 4: ADMET properties of 6 derivatives of Alstiphyllanine A, Alstiphyllanine H and Picrinine

Ligands	Carcinogenicity	Cardiotoxicity	Nephrotoxicity	Acute oral toxicity	Hepatotoxicity	AMES Mutagenicity
(1R,9S,10R,12S,13Z,15S,16R,17R,18R)-18-[(2-aminoethanimidoyl)oxy]-13-(2-aminopropylidene)-17-(methoxycarbonyl)-4,5,8-trimethyl-8,15-diazahexacyclo[14.2.1.0^{1},^{9}.0^{2},^{7}.0^{10},^{15}.0^{12},^{17}]nonadeca-2(7),3,5-trien-15-ium-15-olate	NO	YES	NO	3	YES	NO
(1R,9S,10R,12S,13Z,15S,16R,17R,18S)-13-ethylidene-18-hydroxy-18-(hydroxymethyl)-3,4,8-trimethyl-17-[(trihydroxymethoxy)methanimidoyl]-8,15-diazahexacyclo[14.2.1.0^{1},^{9}.0^{2},^{7}.0^{10},^{15}.0^{12},^{17}]nonadeca-2(7),3,5-trien-15-ium-15-olate	NO	YES	NO	3	NO	NO
aminomethyl (1S,9R,11R,14E,15R,17R,19R)-4,5,6-triamino-14-ethylidene-18-oxa-2,12-diazahexacyclo[9.6.1.1^{9},^{15}.0^{1},^{9}.0^{3},^{8}.0^{12},^{17}]nonadeca-3(8),4,6-triene-19-carboxylate	NO	NO	YES	3	YES	NO
hydrazinylmethyl (1S,9R,11R,14E,15R,17R,19R)-14-ethylidene-4,7-dihydroxy-18-oxa-2,12-diazahexacyclo[9.6.1.1^{9},^{15}.0^{1},^{9}.0^{3},^{8}.0^{12},^{17}]nonadeca-3(8),4,6-triene-19-carboxylate	NO	NO	YES	3	NO	NO
trihydroxymethyl 14-acetyl-4-methyl-18-oxa-2,12-diazahexacyclo[9.6.1.1^{9},^{15}.0^{1},^{9}.0^{3},^{8}.0^{12},^{17}]nonadeca-3,5,7-triene-19-carboxylate	NO	NO	YES	3	YES	NO
hydroxymethyl (14E)-14-ethylidene-5-hydroxy-18-oxa-2,12-diazahexacyclo[9.6.1.1^{9},^{15}.0^{1},^{9}.0^{3},^{8}.0^{12},^{17}]nonadeca-3,5,7-triene-19-carboxylate	NO	YES	YES	3	NO	NO

DISCUSSION

A total of 50 ligand derivatives of Alstiphyllanine A, 50 ligand derivatives of Alstiphyllanine H and 50 ligand derivatives of Picrinine were derived using ACD/ChemSketch software and converted to PDB format using OPEN BABEL software. The results of rough docking using Autodock Vina from PyRx showed that six ligands were fit with a low binding energy.

[Table 1] shows the results obtained in rapid virtual screening by PyRx of SGLT2 and the six ligands. From the table it is clear that the six ligands have low total binding energies and hence were taken for further docking studies. [Figure 5] shows their docking poses in Biovia Discovery Studies window containing the superposed ligands, in 3D, with H-bonds added in green.

The structure and IUPAC names of the three ligands are displayed in [Figure 6].

Accurate docking for the selected six ligands is done using Autodock Vina software in PyRx.[17] The results of docking showing binding affinities of the 6 derivatives of Alstiphyllanine A, Alstiphyllanine H and Picrinine with SGLT2 are displayed in Table 2.

[Table 3] shows the hydrogen bonds, the amino acid residues and its position in the protein involved in the hydrogen bond formation for each ligand docking.

[Table 4] shows the ADMET properties as well as mutagenicity, carcinogenicity of the six ligands. It was determined by using ADMETSAR online tool.[18] The drug likeness was determined using

ISSN (O): 2687-5365; ISSN (P): 2753-6556

SwissADME software.[19] They all possess good drug likeness.

The six ligands, have excellent binding energy with good ADMET properties.

The early identification of drug side effects is of high interest in drug discovery. Most of the drugs fail clinical trials because of side effects deriving from unexpected interactions. Pharmacovigilance is also important because they reveal potential safety risks that often could not be detected within clinical trials. Several computational approaches are available to assist this task which require a satisfactory amount of bioactivity data, or already reported adverse effects. The major advantage of molecular docking is that it needs only the structural information of the targets to perform its predictions. Therefore, it is a valuable approach to predict potential side effects of compounds at an early phases of clinical developments.[13]

The reliability of docking protocols has improved constantly. The most recent implementations address quite efficiently some classic shortcomings of the technique. Enzymatic bioassays, in vivo animal studies primarily in rodents make a study more accurate and reliable. But important breakthroughs are expected thanks to the ever-increasing computational power of multicore CPUs.[14]

CONCLUSION

The results of docking showed that all the six ligands had lower binding energies than docking binding energy of empagliphlozin with the SGLT2 except one ligand ((1R,9S,10R,12S,13Z,15S,16R,17R,18R)-18-[(2-aminoethanimidoyl)oxy]-13-(2-aminopropylidene)-17-(methoxycarbonyl)-4,5,8-trimethyl-8,15 diazahexacyclo[14.2.1.0^{1},^{9}.0^{2},^{7}.0^{10},^{15}.0^{12},^{17}]nonadeca-2(7),3,5-trien-15-ium-15-olate) which has the same binding energy as Empagliflozin. The other five out of the six ligands exhibited strong binding with SGLT2 with binding energies values of -8, -8.5, -8.6, -8.7 and -9.2 kcal/mol for SGLT2 which is lower than that of the binding energy of empagliflozin with SGLT2 which is -6.78kcal/mol thus making these ligands more potent inhibitors of SGLT2 than Empagliphlozin. Also, the physiochemical properties showed that these compounds have good drug-likeness and this study is done by the directly docking SGLT2 with the selected ligands in comparison with other previous studies which are done by homology modelling making the results more accurate (15). Therefore, if these compounds are investigated further, they might be potential SGLT2 inhibitors with lesser adverse effects and better outcomes(16).

REFERENCES

1. Wakisaka M, Kamouchi M, Kitazono T. Lessons from the Trials for the Desirable Effects of Sodium Glucose Co-Transporter 2 Inhibitors on Diabetic Cardiovascular Events and Renal Dysfunction. Int J Mol Sci. 2019 Nov 12;20(22):E5668.
2. Cole JB, Florez JC. Genetics of diabetes and diabetes complications. Nat Rev Nephrol. 2020 Jul;16(7):377–90.
3. Davidson JA, Kuritzky L. Sodium glucose co-transporter 2 inhibitors and their mechanism for improving glycemia in patients with type 2 diabetes. Postgrad Med. 2014 Oct;126(6):33–48.
4. Hsia DS, Grove O, Cefalu WT. An Update on SGLT2 Inhibitors for the Treatment of Diabetes Mellitus. Curr Opin Endocrinol Diabetes Obes. 2017 Feb;24(1):73–9.
5. Andreea MM, Surabhi S, Razvan-Ionut P, Lucia C, Camelia N, Emil T, et al. Sodium-Glucose Cotransporter 2 (SGLT2) Inhibitors: Harms or Unexpected Benefits? Medicina (Mex). 2023 Apr;59(4):742.
6. Taylor SI, Blau JE, Rother KI. SGLT2 Inhibitors May Predispose to Ketoacidosis. J Clin Endocrinol Metab. 2015 Aug;100(8):2849–52.
7. Singh M, Kumar A. Risks Associated with SGLT2 Inhibitors: An Overview. Curr Drug Saf. 13(2):84–91.
8. Arai H, Hirasawa Y, Rahman A, Kusumawati I, Zaini NC, Sato S, et al. Alstiphyllanines E-H, picraline and ajmaline-type alkaloids from Alstonia macrophylla inhibiting sodium glucose cotransporter. Bioorg Med Chem. 2010 Mar 15;18(6):2152–8.
9. Morris GM, Lim-Wilby M. Molecular docking. Methods Mol Biol Clifton NJ. 2008;443:365–82.
10. ACD/Labs [Internet]. [cited 2022 Nov 3]. Free Chemical Drawing Software for Students | ChemSketch. Available from: https://www.acdlabs.com/resources/free-chemistry-software-apps/chemsketch-freeware/
11. Morris GM, Huey R, Lindstrom W, Sanner MF, Belew RK, Goodsell DS, et al. AutoDock4 and AutoDockTools4: Automated docking with selective receptor flexibility. J Comput Chem. 2009 Dec;30(16):2785–91.
12. Cheng F, Li W, Zhou Y, Shen J, Wu Z, Liu G, et al. admetSAR: A Comprehensive Source and Free Tool for Assessment of Chemical ADMET Properties. J Chem Inf Model. 2012 Nov 26;52(11):3099–105.
13. Pinzi L, Rastelli G. Molecular Docking: Shifting Paradigms in Drug Discovery. Int J Mol Sci. 2019 Jan;20(18):4331.
14. Bottegoni G. Protein-ligand docking. Front Biosci Landmark Ed. 2011 Jun 1;16(6):2289–306.
15. Subbiah U, Ajith A, Venkata Subbiah H. Molecular docking and dynamics simulation of Orthosiphon stamineus against SGLT1 and SGLT2. J Biomol Struct Dyn. 2023;41(23):13663–78.
16. Abdulaal WH, Bakhrebah MA, Nassar MS, Almazni IA, Almutairi WA, Natto ZS, et al. Insights from the molecular docking analysis of SGLT2 and FIMH to combat uropathogenicity. Bioinformation. 2022 Nov 30;18(11):1044–9.

ISSN (O): 2687-5365; ISSN (P): 2753-6556